608463

RECENT LOADS CALIBRATION EXPERIENCE WITH A DELTA WING AIRPLANE

by

Jerald M. Jenkins

and

Albert E. Kuhl

To be Presented at

Fall Meeting

Western Regional Strain Gage Committee

Society for Experimental Stress Analysis

September 28, 1977

NASA Dryden Flight Research Center

Edwards, California

INTRODUCTION

Aircraft which are designed for supersonic and hypersonic flight are evolving with delta wing configurations (ref. 1-3). An integral part of the evolution of all new aircraft is the flight test phase. Included in the flight test phase is an effort to identify and evaluate the loads environment of the aircraft. The most effective way of examining the loads environment is to utilize calibrated strain gages (ref. 4) to provide load magnitudes. Using strain gage data to accomplish this has turned out to be anything but a straightforward task. The delta wing configuration has turned out to be a very difficult type of wing structure to calibrate. Elevated structural temperatures result in thermal effects (ref. 5) which contaminate strain gage data being used to deduce flight loads. The concept of thermally calibrating a strain gage system is an approach to solving this problem (ref. 6).

This paper will address how these problems were approached on a program (ref. 7-8) directed toward measuring loads on the wing of a large, flexible supersonic aircraft. Structural configurations typical of high-speed delta wing aircraft will be examined. The temperature environment (ref. 9-10) will be examined to see how it induces thermal stresses which subsequently cause errors in loads equations used to deduce the flight loads. A heating test of a delta wing airplane will

be presented which demonstrates the concept of a thermal calibration. The use of simple structural computer models to predict strains (ref. 11) will be shown to be an asset in terms of locating strain gages and in developing load equations. The general philosophy of calibrating delta wing aircraft will be discussed and the approach used to determine the accuracy of an equation will be examined.

STRUCTURAL CONFIGURATIONS

Wings, which are configured for supersonic and hypersonic flight, have characteristics tailored to both aerodynamic and structural considerations. The frequently conceived delta wing shape reflects a desire for aerodynamic efficiency. Structural considerations are generally latent and require considerable explanation. Shown in Figure 1 is a structural skeleton of a delta wing airplane. The wing surfaces are built up of a beaded outer skin and corrugated inner skin. These surfaces are supported by 28 closely spaced spanwise beams and by four chordwise ribs. The wing beams are continuous through the fuselage. An engine nacelle is an integral part of the wing and nacelle rings provide continuity between the inner wing and outer wing beams. The information in this paper centers around tests and analysis on this configuration. The unique additional factor to the structural design of a

supersonic or hypersonic wing is the presence of elevated structural temperatures and the related temperature gradients. Differential temperatures among structural elements, dissimilar materials, and nonlinear temperature distributions result in thermal stresses that can be of very large magnitudes.

There is little documented knowledge about the state-of-the-art of calculating thermal stresses in complex structures. This deficiency has probably led to avoidance design philosophies. The designer has chosen to configure the structure such that thermal stresses are avoided as much as possible. An example of this avoidance design is illustrated in Figure 2. It can be seen that the skins have a corrugated type of fabrication to allow expansion in one direction. It can also be seen that these skins are attached to the substructure using a stand-off type of clip. This type of configuration allows expansion to be absorbed in a manner similar to the displacement of an accordian. The standoff clips provide the structural continuity without unneeded restraint. The standoff clips also minimize the heat conduction paths so that there is a heat shield effect.

Another example of avoidance design (ref. 12) is seen in Figure 3. This wing structure is typical of hot, radiating wing structures which are envisioned for hypersonic flight. This configuration specifically has a heat shield for thermal

protection of the substructure elements. Beaded panels are utilized to provide thermal growth capability in the chord direction while at the same time providing efficient buckling strength in the span direction. Sine-wave spars are also included in the design. This allows the spars to deform longitudinally in response to the exterior structures' thermal growth, but still providing very good vertical shear capability.

It is very likely that designs of the future will include such avoidance techniques as has been discussed. This will tend to reduce the magnitudes of thermal stresses, but not eliminate them, as will be shown later.

THERMAL ENVIRONMENT

The temperature environment resulting from aerodynamic heating is a major subject in itself. The primary problems arising from elevated structural temperatures have to do with the structure itself. There are two important factors which must be considered: (1) the absolute magnitude of the temperature, and (2) the manner in which the temperature is distributed. The absolute temperature magnitude affects such things as the strength of the material, the stiffness of the material, and the interactions between dissimilar materials. The temperature gradients and the nature of the gradients affects primarily the severity of the thermal stresses.

These factors do influence how and whether flight loads can be acquired with strain gages.

The isotherms shown in Figure 4 illustrate how steady state temperatures are distributed on a supersonic airplane cruising at Mach 3. It can be seen that maximum temperatures reach 600^{o} F. The manner in which these temperatures increase is shown in Figure 5 at three different skin locations. It can be seen that as the airplane increases speed to its Mach 3 cruise, the skin temperatures continue to rise and very quickly reach steady state as the cruise condition is attained.

Although the skin areas do generally reach steady state temperatures quickly, this is not true of the substructure. Shown in Figure 6 is a time history illustrating that the substructure spar cap and spar web take a long time to reach steady state temperature. The airplane cruises at Mach 3 for fifteen minutes before the substructure temperatures begin to stabilize. This effect can be more graphically seen in Figure 7. The temperatures are plotted for four different time segments during a Mach 3 cruise flight. Very early in the flight (time = 8 minutes), it can be seen that the temperature gradients are large and the distribution of temperature is highly nonlinear. As the temperature reaches steady state (time = 32 minutes), it can be seen that the gradients are not large and the nonlinearity is significantly reduced.

The nature of these gradients and the character of the nonlinearities has great impact on the thermal stress patterns induced in the aircraft structure by the temperature field. Transient thermal stresses will be a major design in any supersonic aircraft having capabilities of speeds much above Mach 2. The presence of these thermal stresses also affect strain gages which were, for instance, intended to measure stresses due to aerodynamic, inertial, or dynamic loads. These thermal stresses can lead to a major source of error if they are not considered in strain gage calibration procedures.

THERMAL STRESSES

There are two types of thermal stresses that must be considered within the scope of this paper. The first type (ref. 13) of thermal stresses result from the forces that arise in a system of mutually connected members as a result of their combined effect on one another either fron nonuniform thermal action on the bodies making up the system, or from having different coefficients of expansion, such as might occur when several spars in an airplane wing are at different temperatures. The second type (ref. 13) of thermal stresses result from non-linearities in the temperature field or in the material properties of the body such as might occur if a single spar had a non-linear temperature gradient through its depth. These types of thermal stress are a direct result of the supersonic aircraft environment.

As an illustrative example, consider the structural element in Figure 8. If the temperature distribution shown is imposed on this skin/substructure element, then the thermal stresses arise due to the nonlinear nature of the temperature distribution. Thermal stresses may be computed using elementary beam theory (ref 14).

The results of this type of thermal stress analysis is shown in Figure 9. The stress pattern in the skin reflects the heat sink effect of the substructure. Tensile stresses exist in the cooler areas near the substructure and compressive stresses exist in the hotter areas. A widely varying stress pattern is also seen through the depth of the substructure. Large tensile stresses exist in the web area while the lower cap has compressive stresses. It can easily be seen that the thermal stresses are widely varying in distribution. Further investigation would likely lead to the conclusion that a fairly laborious analysis is required before enough information is available to plan scientific endeavors which are affected by thermal stresses.

It is very important to understand that the distribution of thermal stress shown in Figure 9 is for a single instant in time. Thermal stresses are for the most part time dependent. Since thermal stresses are induced by the temperature field, the thermal stresses vary in time in direct relation to the way the temperatures vary in time. If Figure 6 is recalled,

it can be seen that the temperatures are changing the majority of the time. So when the heating and cooling cycles are considered, thermal stresses at any one discreet element may vary from large compressive to large tensile values during a flight.

An illustrative example of the transient behavior of strain gages can be seen indirectly in Figure 10. In order to more graphically explain the content of Figure 10, it is necessary to define what a load equation is. A load equation is a linear equation relating several strain gages to a set of calibration loads (ref. 4). The data presented in Figure 10 was developed by performing a heating simulation in a laboratory on the airplane shown in Figure 1. This ground heating allowed the determination of the strain gage outputs due to the effects of heat alone. These outputs could then be put into the load equation and a thermal load could be calculated. The thermal load is really a ficticious number which represents the error in the load equation due to heating effects. So, a time history of the thermal error is shown in Figure 10 for a shear, a bending, and a torsion equation. This error is primarily, but not exclusively, caused by thermal stresses. The thermal load is shown as a ratio with respect to a reference load. The reference load is a value which corresponds closely to a one "g" wing loading. It is shown in

this manner to give the reader a feel for the relative magnitude of the thermal effects.

It can be seen that the responses of the strain gages in the shear and torque equations maximize near the time the cruise at Mach 3 begins. This value approaches half of the reference load. This correlates with the nonlinear distributions of temperature shown in Figure 7. The nonlinearity of the temperature distribution has the greatest effect on the web thermal stresses which are primarily used to develop shear and torsion equations.

The time history of the bending equation is quite different in nature. It can be seen that it slowly builds up to around 10 percent of the reference load near the end of the cruise. The bending gages, which are usually located on the caps or skins, may be more sensitive to the temperature rise rather than thermal stress levels.

THERMAL CALIBRATION

The effect of temperature has been presented clearly in the preceeding sections. The presence of thermal stresses of unknown magnitudes in the region where strain gages are located leads to the problem of the strain gages sensing both aerodynamic forces and thermal effects. This problem is similar to the situation that arises when loads are

measured during conventional subsonic maneuvering flight. In this case, the strain gages sense a conglomerate of aerodynamic loads and inertial loads. The total measured load, L_M, is a combination of aerodynamic forces, L_A, and inertial forces, L_I, i.e.,

$$L_M = L_A + L_I$$

Since inertial loads can be calculated quite accurately if the mass characteristics of a wing are known, the aerodynamic load can be calculated by deducting the calculated inertia load from the total measured load, i.e.,

$$L_A = L_M - L_I$$

This is a commonly used correction approach used to remove inertia load from flight data. The same type of relationship is valid for removing thermal effects of supersonic and hypersonic maneuvering flight, i.e.,

$$L_A = L_M - L_T - L_I$$

where L_T is the ficticious load induced by thermal effects. The philosophy of the correction is straightforward. Implementing the correction is not, however, because determining the value of L_T is a very complex problem. The thermal effect, L_T, is a large number frequently, and it must be determined with substantial accuracy. The ideal way of determining the thermal effects would be to calculate the thermal stresses. There is very little information available on the

state-of-the-art of calculating thermal stresses in complex structures. The meager information (ref. 15) that is available indicates large deviations between predicted and measured values. Precise calculations of thermal stresses also requires a thorough and detailed definition of structural temperatures. Such a calculation would be awesome in size. It does not appear that calculating thermal stresses is a viable way of providing a correction unless considerable progress is made in calculative techniques.

Another approach that is more straightforward is a procedure known as a thermal calibration. The procedure is to heat the structure of the airplane in a ground-based facility to the identical conditions experienced during a flight. The object is to obtain thermal outputs from each of the strain gages due to heating effects only. There are no aerodynamic or other external forces (gravity excepted) present to contaminate the determination of the thermal effects. This type of calibration was performed on the airplane discussed in this paper, and the results were presented at a national symposium in 1974 (ref. 16). The thermal calibration approach has been demonstrated to be a feasible one. However, the task of performing a thermal calibration is quite formidable. Duplicating an inflight temperature time history for a complex airplane structure

is time consuming, costly, and technically complex. The heating of the airplane to obtain a thermal calibration is shown in Figure 11. The heating was accomplished by controlling the airplane's surface temperatures with thermocouples linked to a digital computer which commanded heating inputs from banks of radiant heat lamps. The surface of the airplane was divided into approximately 1000 zones which were controlled independently during the thermal calibration. The heating time histories of several flight profiles were simulated for use as corrections for several high Mach number conditions. This information was then used to correct flight data.

There are characteristics which should be known when thermal calibrations are necessary. The anatomy of a supersonic flight from the thermal aspect is shown in Figure 12. There are three distinct phases of a flight: (1) increasing Mach number, (2) cruise at constant Mach number, and (3) decreasing Mach number. Temperature time histories of typical skin and web responses are shown. For the majority of the flight, the structure is in a state of changing temperature. As was discussed in Figures 5-10, the largest thermal stresses (which result in the largest thermal corrections) occur during the transient portion of the flight. This means that when the temperatures are near steady state,

the thermal corrections are at their smallest values. This is depicted in Figure 13. Early in the flight, the thermal component (or thermal correction) is large compared to the aerodynamic component of load. When the ratio of L_T/L_A is large there is more chance for error just by virtue of the size of the correction. When the ratio of L_T/L_A is small, such as for maneuver B, the minor errors in determining the correction have much less impact on determining the aerodynamic component accurately. It is, therefore, preferable to conduct loads maneuvers when the thermal gradients are small and when the temperature is near an equilibrium situation.

If there are special interests, such as high airplane gross weight data then this information cannot be obtained during the latter part of a flight. It also must be considered that as a flight progresses, the constant "g" wing loads decrease because the gross weight is decreasing due to fuel consumption. This could effect the L_T/L_A ratio. So, it can be concluded that although it is preferable to get data late in the flight, there are exceptions to this approach.

LOAD CALIBRATIONS

The traditional approach used on obtaining loads from calibrated strain gages on wings, in general, has followed a sequence that includes: (1) locating strain gage bridges on

pertinent structural members, (2) applying point loads to the wing in a grid pattern, (3) linearly relating the applied loads to the strain gage bridge outputs in the form of an equation, and (4) computing an equation error by inputting the strain gage bridge outputs for each load condition into the equations and calculating the variance from the known applied load. This approach has been used for decades on high aspect ratio wings with great success. However, delta wing shapes are not so amenable to this approach. In fact, there is virtually no information available to use as a guide for calibrating delta wing airplanes. However, recent experience has provided some information pertinent to this problem.

The basic problem is that delta wings usually are multi-spar configurations with large chord dimensions relative to the span dimensions. This means that with many load paths and much structural redundancy, it is difficult to determine how well a system can measure various load distributions. A study was conducted with two objectives: (1) to study a computational approach to evaluating equation suitability with respect to the flight load variation to be measured, and (2) to study how well simple computer structural models can be used to predict load response characteristics.

Mathematical Loadings - In order to develop a technique

of evaluating how accurately a load equation can be used to measure various load distributions, it is necessary to identify a range of load distributions to serve as the standard. The three load distributions shown in Figure 14 represent a reasonable cross section of expected loadings. Included is a loading with a forward center of pressure (typical of a subsonic load distribution), a loading with a central center of pressure (typical of a supersonic load distribution), and an aft center of pressure loading (typical of a loading induced by a large control surface deflection).

A plan is schematically diagrammed in Figure 15 for interfacing the three mathematical loadings with the information developed from the load calibration. The load calibration provided influence coefficients and load equations. If the three mathematical loadings are subdivided into local area loadings which correspond to the calibration load points, then a strain gage bridge output can be calculated by multiplying the local area loading by the influence coefficient for that area. If this is done for all the local area loadings and if all of the resulting outputs are summed, then the result is the total output for each strain gage bridge due to that total mathematical wing loading. If these outputs are used appropriately in the load equations, then a load may be calculated for comparison with the mathematically applied

loading. This is a type of functional check on how the load measuring system responds to varying load distributions.

This approach was used to examine the load calibration and the subsequently developed load equations of the delta wing aircraft of Figure 1. A mathematical loading of 10,000 pounds was distributed over the surface of the wing according to the three load distributions (ref. 17-19) shown in Figure 14. The procedures outlined in Figure 15 were then used to calculate the loads from the superimposed strain gage outputs and the available load equations. The results are shown in Figures 16, 17, and 18.

In Figure 16, eight shear equations were checked using the above mentioned procedure. It can be seen that many of the equations calculate a load less than the mathematically applied one. This implies a deficiency in the equation's ability to account for all the load on the surface. The worst case was the aft center of pressure case where deficiencies of 20 percent or more were the rule.

The bending moment results shown in Figure 17, show a different trend. The greatest deficiency shows up in the central center of pressure case where the deficiency is between five and 10 percent. The bending moment equations, in general, seemed quite consistent and able to accommodate load variations well.

Six torsion equations are examined in Figure 18. Extreme caution must be exercised when examining torsion data since the reference axis location is arbitrary and this affects the magnitude of the results. The reader is cautioned that the vertical scales are different for the three cases. The results, however, do indicate a large discrepancy between the calculated load and the applied load for the aft center of pressure case. There are equations in the other two cases which do calculate loads reasonably close to the mathematically applied load.

There are two basic conclusions that can be drawn from this study: (1) there is still a great deal we do not understand about calibrating delta wings, and (2) computational procedures can obviously be a great aid in equation selection and in system error evaluations.

Another interesting feature can be seen in Figure 19. The location of the calibration loads is shown and the length of the vector represents the magnitude of the load. It is curious to note that there is little correlation between the location of the large calibration loads and the location of the large flight loads (Figure 14). The magnitude of the calibration loads are usually dictated by substructure bearing strength. This does not necessarily correspond to the way loads are distributed on the wing surface. This is a

very typical and common circumstance, particularly on delta wings.

Structural Computer Models - It would be of great advantage to know the nature of structural response of various wing spars prior to developing a load calibration plan. A study was conducted to determine if a relatively simple structural model could be used to predict spar strain responses to load and to develop predicted influence coefficient plots of a general nature. The study was limited to a simple structural model since a point of diminishing returns is quickly reached when the expense of modeling is considered.

A bar element NASTRAN model of the wing of the supersonic aircraft of Figure 1 was developed to conduct this study. The ability of the model to predict strains along the root of the wing is shown in Figures 20 and 21. In Figure 20, calculated and measured shear strains are shown at the wing root spars for loads applied to the wing at the location and in the direction of the arrows. It can be seen that the correlation between the measured shear strains and the strains calculated using the simple computer model is quite good. A similar comparison is made in Figure 21 for bending strains. It can also be seen that the correlation between measured and predicted strains is quite good.

In Figures 22 and 23, influence coefficients have been calculated using the structural model and they have also been calculated from the laboratory load calibration data. The influence coefficients represent the strain per unit applied load. The influence coefficient is plotted against the span on the basis of constant chord lines. The measured and calculated influence coefficients are compared in Figure 22 for three different shear bridges located strategically along the wing root. It can be seen that the characteristic shapes of the measured and calculated curves are quite similar. In one case, (a), the magnitude of the calculated data exceeds the measured data considerably. However, the general correlation is quite good. A similar comparison is shown in Figure 23 for a bending bridge. The correlation for bending bridges was quite good and this plot is typical.

The results of this study indicate that considerable information can be gained from a simple structural computer model of this supersonic wing. This type of information could prove invaluable for locating strain gages and for identifying potential strain gage combinations for load equations.

CONCLUDING REMARKS

Wing configurations for supersonic and hypersonic airplanes are contemplated as low aspect ratio structures

with delta-wing shapes occurring the most frequent. The trend in design has been to configure the structure so that large thermal stresses are avoided. However, since there is no practical way to eliminate thermal stresses, they must be considered in all functional aspects of an airplane.

All aircraft which encroach very far into the supersonic/hypersonic speed range experience the effects of aerodynamic heating. Both high temperatures and large thermal gradients affect the validity of load measurements with calibrated strain gages. Structural temperature levels may become high enough to alter spar stiffness which could result in load path changes which could subsequently invalidate the wing strain gage calibration. Nonuniform temperature distributions induce thermal stresses which can be very large and can contaminate flight measurements of loads using strain gages.

Thermal effects which prohibit obtaining valid high Mach number strain gage data can be accounted for by thermally calibrating supersonic airplanes. A ground laboratory heating is a necessary part of the flight test program, if valid loads data are to be obtained. Thermal effects vary in size during supersonic flights, but they are large enough to require accounting at all times.

A study to examine the adaptability of a set of loads equations selected solely on the basis of the loads calibration revealed that discrepancies can exist if the load to be measured is not considered in the overall selection process. The results of a study indicated that a relatively simple structural computer model can be very useful in predicting strain response to external loads with relatively good accuracy. This capability provides considerable foresight in locating strain gages and in identifying possible strain gage combinations for use in load equations.

REFERENCES

1. Jenkins, Jerald M.; DeAngelis, V. Michael; Friend, Edward L.; and Monaghan, Richard C., "Flight Measurements of Canard Loads, Canard Buffeting, and Elevon and Wing-Tip Hinge Moments on the XB-70 Aircraft Including Comparisons with Predictions," NASA TN D-5359, August, 1969.

2. Rich, Ben R., "The F-12 Series Aircraft: Aerodynamic and Thermodynamic Design in Retrospect," AIAA Paper No. 73-820, AIAA 5th Aircraft Design, Flight Test, and Operations Meeting, St. Louis, Missouri, August 6-8. 1973.

3. Ripley, E. L., "Structural Tests for the Supersonic Transport Aircraft," Technical Report 70121, Royal Aircraft Establishment, July, 1970.

4. Skopinski, T. H.; Aiken, W. S., Jr.; and Huston, W. B., "Calibration of Strain-Gage Installations in Aircraft Structures for the Measurement of Flight Loads," NACA Report No. 1178, 1954.

5. Jenkins, Jerald M.:Some Views on the Use of Strain Gages for Flight Loads Measurements on Future High Performance Aircraft. Proceedings of Western Regional Strain Gage Committee-1969 Spring Meeting, Philip O. Vulliet, ed., pp. 1-2.

6. Fields, Roger A., "Strain Gage Measurement of Flight Loads at Elevated Temperature", NASA YF-12 Flight Loads Program, NASA TM X-3061, May 1974.

7. Sefic, W. J.; and Reardon, L. F., "Loads Calibration of the Airplane," NASA YF-12 Flight Loads Program, NASA TM X-3061, May, 1974.

8. Jenkins, J. M.; and Kuhl, A. E., "Summary of Recent Results Pertaining to Strain Gage Load Measurement Technology on High-Speed Aircraft," NASA YF-12 Flight Loads Program, NASA TM X-3061, May, 1974.

9. Quinn, Robert D.; and Olinger, Frank V., "Flight Temperatures and Thermal Simulation Requirements," NASA YF-12 Flight Loads Program, NASA TM X-3061, May, 1974.

10. Olinger, Frank V.; Sefic, Walter J.; and Rosecrans, Richard J., "Laboratory Heating Tests of the Airplane," NASA YF-12 Flight Loads Program, NASA TM X-3061, May, 1974.

11. Jenkins, J. M.; Kuhl, A. E.; and Carter, A. L., "The Use of a Simplified Structural Model as an Aid in the Strain Gage Calibration of a Complex Wing," NASA TM X- 56046, July 1977.

12. Plank, P. P.; and Pennings, F. A., "Hypersonic Wing Test Structure Design, Analysis, and Fabrication," NASA CR-127490, August, 1973.

13. Fridman, Ya. B., "Strength and Deformation in Nonuniform Temperature Fields," authorized translation from the Russian Consultants Bureau, New York, 1964.

14. Boley, Bruno A.; and Weiner, Jerome H., "Theory of Thermal Stresses," second edition, John Wiley & Sons, Inc., 1962.

15. Carter, Alan L., "Assessment of Recent Loads Analysis Methods as Applied to a Mach 3 Cruise Airplane," NASA YF-12 Flight Loads Program, NASA TM X-3061, May, 1974.

16. Et al., NASA YF-12 Flight Loads Program, NASA TM X-3061, May, 1974.

17. Allen, J. H., "General Theory of Airfoil Sections Having Arbitrary Shape or Pressure Distribution," NACA Report 883, 1945.

18. DeYoung, J.; and Harper, C. W., "Theoretical Symmetric Span Loading at Subsonic Speeds for Wings Having Arbitrary Plan Form," NACA Report 921, 1948.

19. Tucker, W. A.; and Nelson, R. L., "Theoretical Characteristics in Supersonic Flow of Two Types of Control Surfaces on Triangular Wings," NACA Report 939, 1949.

STRUCTURAL SKELETON OF A COMPLEX DELTA-WING AIRCRAFT

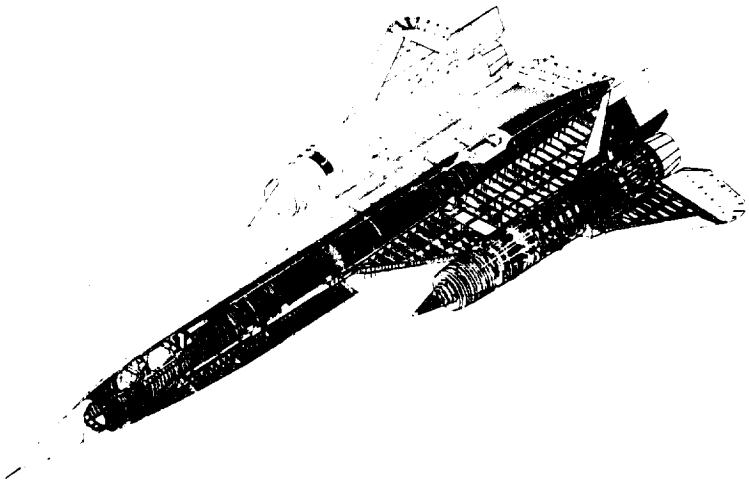

Figure 1

DESIGN USED FOR WING TO MINIMIZE THERMAL STRESS

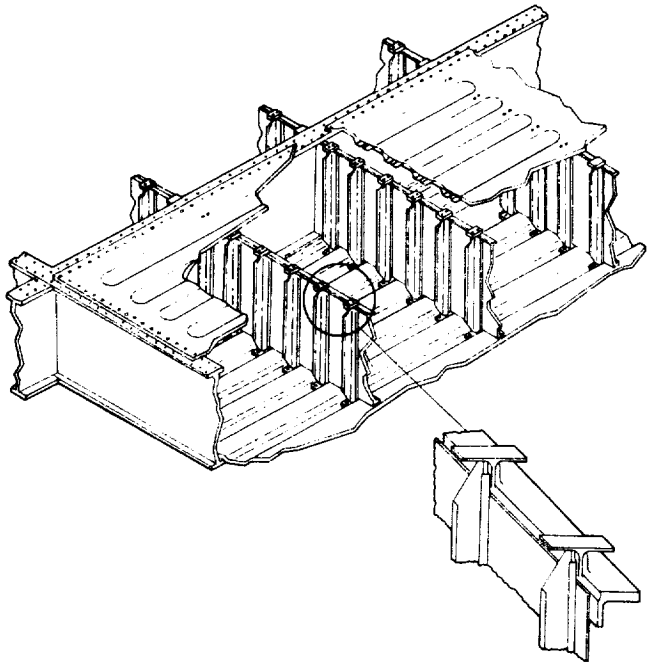

Figure 2

CHARACTERISTICS OF TYPICAL ADVANCED STRUCTURES

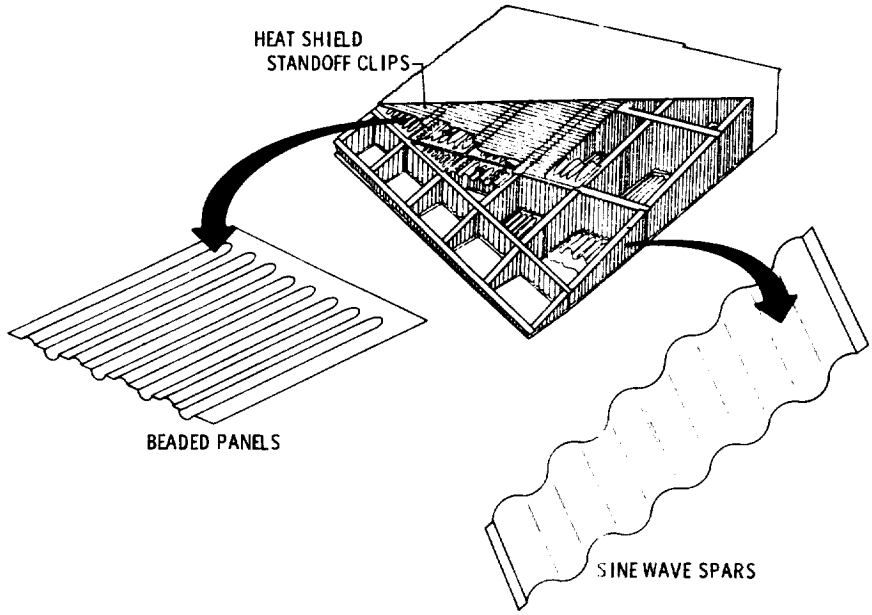

Figure 3

SURFACE TEMPERATURES AT HIGH MACH NUMBER CRUISE CONDITION

[TEMPERATURES ARE IN DEGREES KELVIN (DEGREES FAHRENHEIT)]

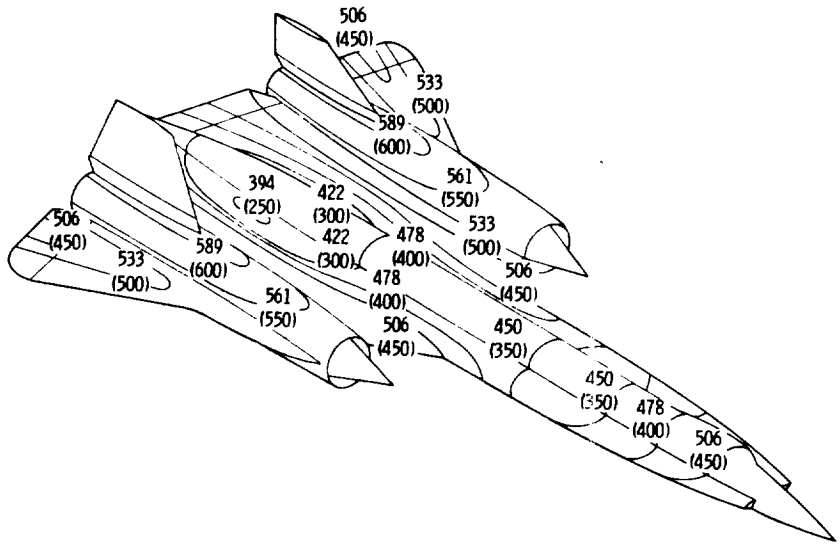

Figure 4

TIME HISTORY OF TYPICAL WING SKIN SURFACE TEMPERATURES

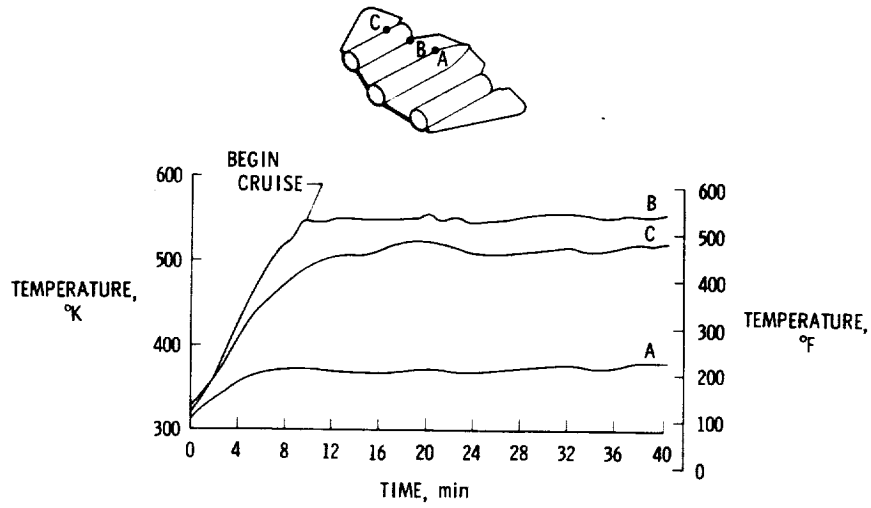

Figure 5

TIME HISTORY OF TYPICAL WING SPAR TEMPERATURE DISTRIBUTION

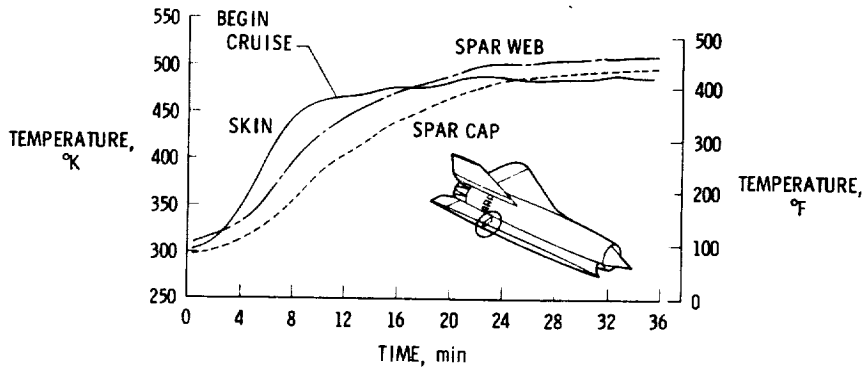

Figure 6

DISTRIBUTION OF TYPICAL TEMPERATURES IN WING SPAR

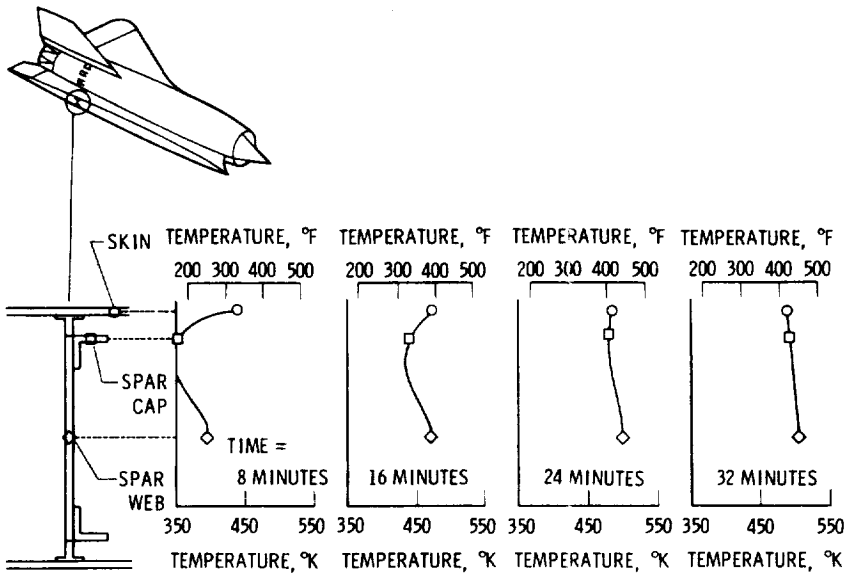

Figure 7

TEMPERATURE DISTRIBUTION FOR ANALYSIS OF SAMPLE BEAM

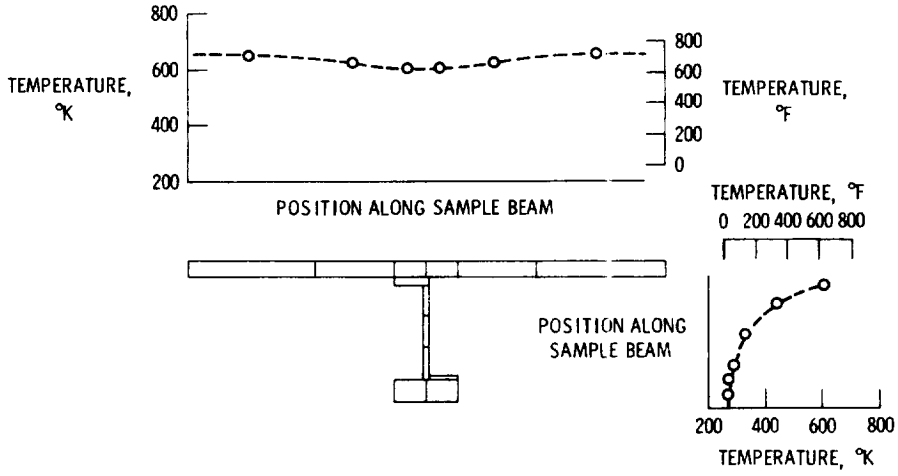

Figure 8

THERMAL STRESS DISTRIBUTION FOR ANALYSIS OF SAMPLE BEAM

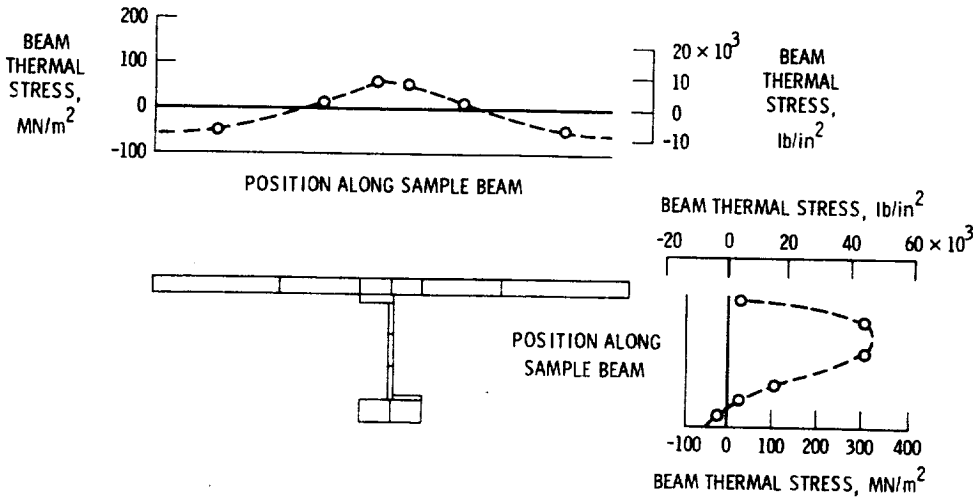

Figure 9

THERMAL EFFECTS ON STRAIN GAGE LOAD EQUATIONS

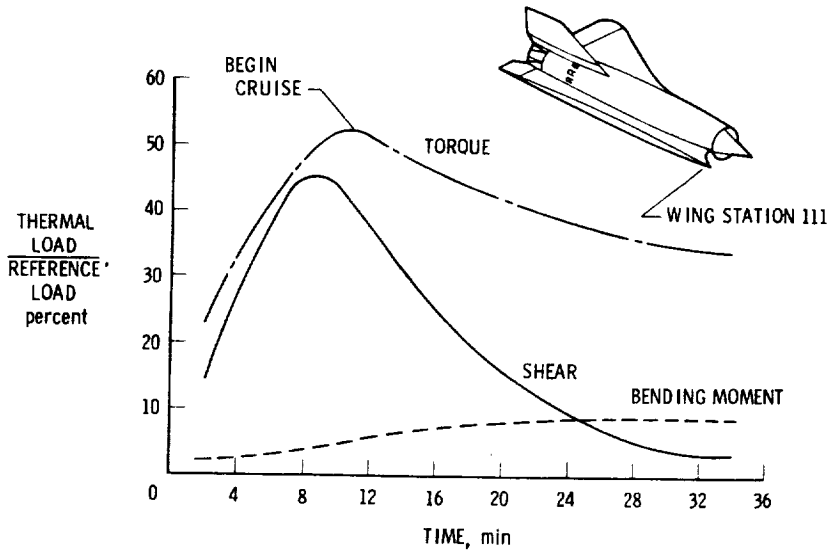

Figure 10

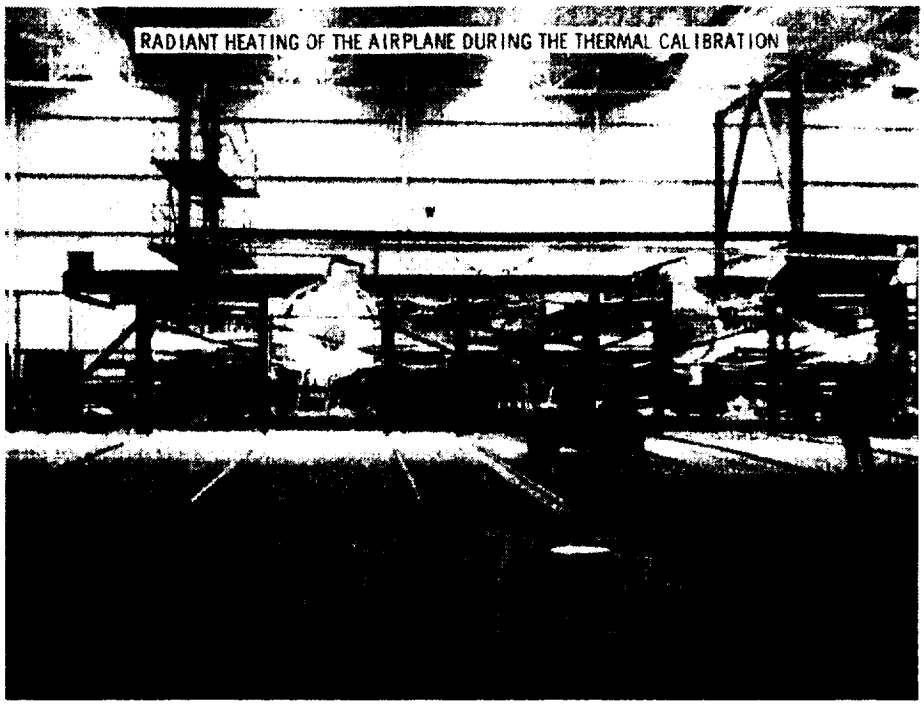

Figure 11

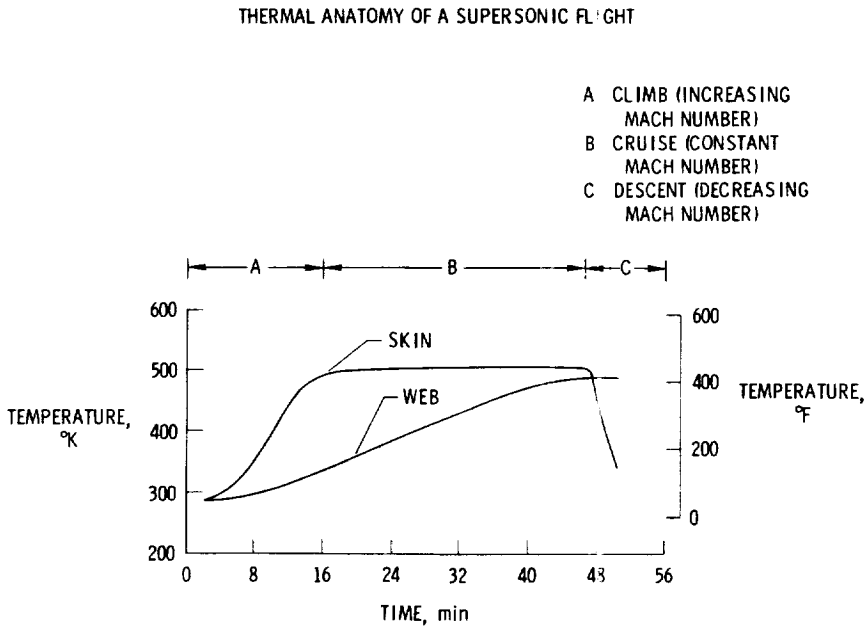

Figure 12

AERODYNAMIC AND THERMAL COMPONENTS OF LOAD RELATIVE TO FLIGHT PROFILE

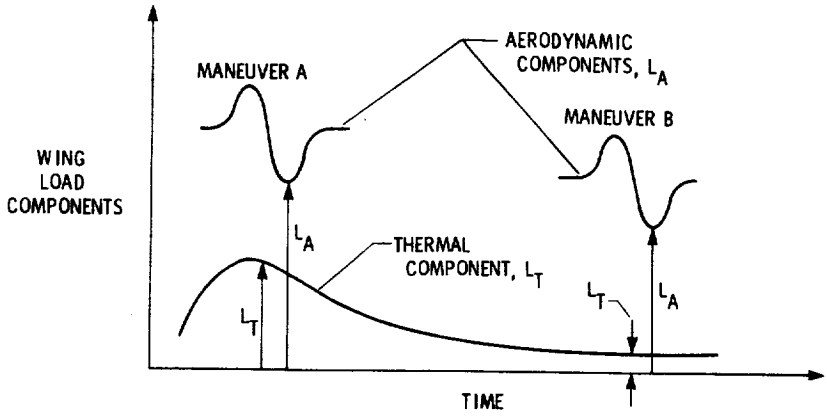

Figure 13

DISTRIBUTION OF MATHEMATICALLY APPLIED LOADS

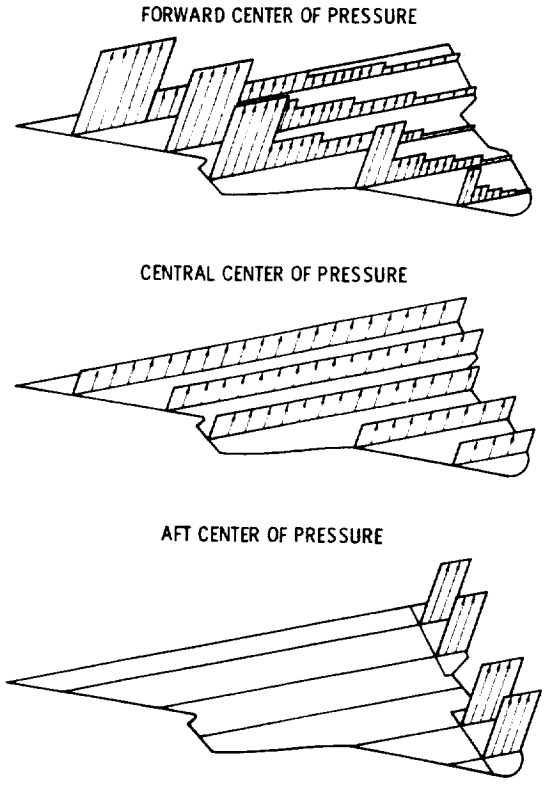

Figure 14

SCHEMATIC OF COMPUTATION OF MATHEMATICALLY APPLIED LOADS

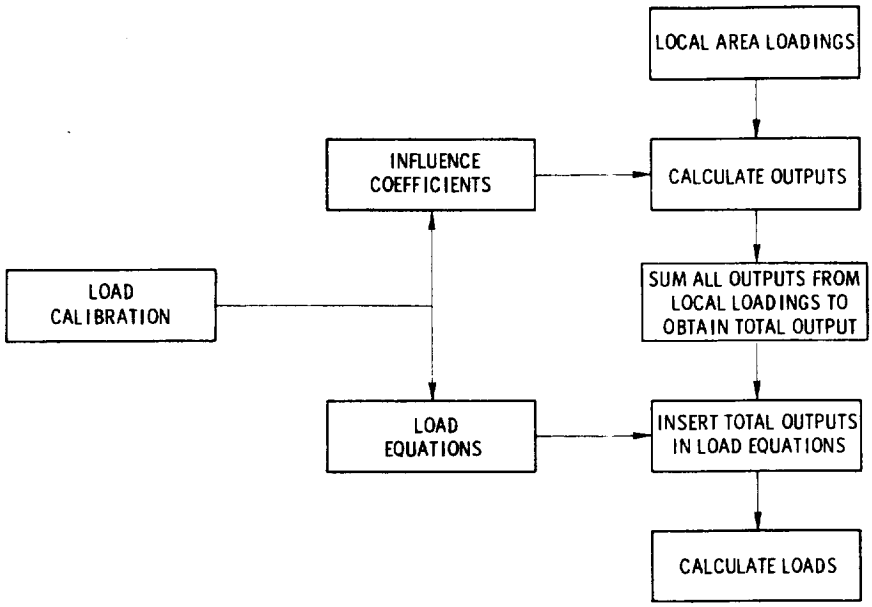

Figure 15

COMPARISON OF CALCULATED AND MATHEMATICALLY APPLIED SHEAR LOADS

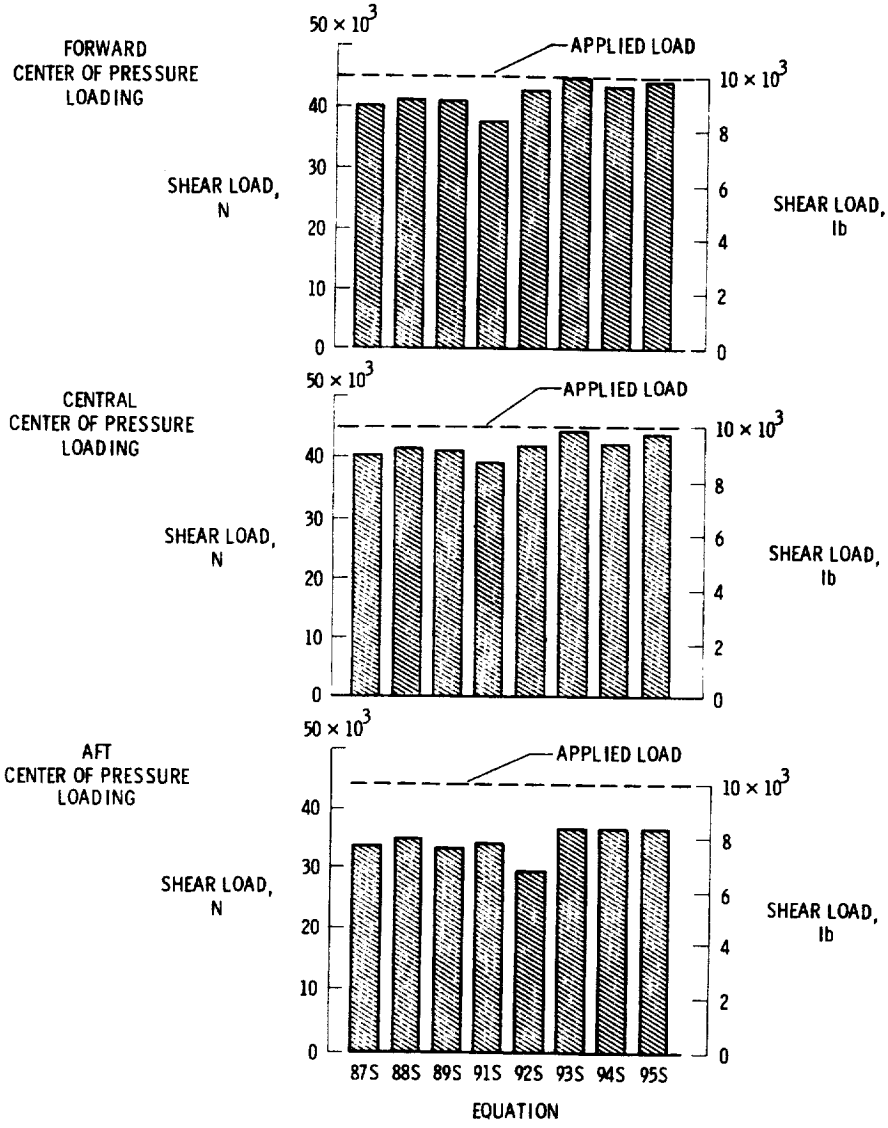

Figure 16

COMPARISON OF CALCULATED AND MATHEMATICALLY
APPLIED BENDING MOMENTS

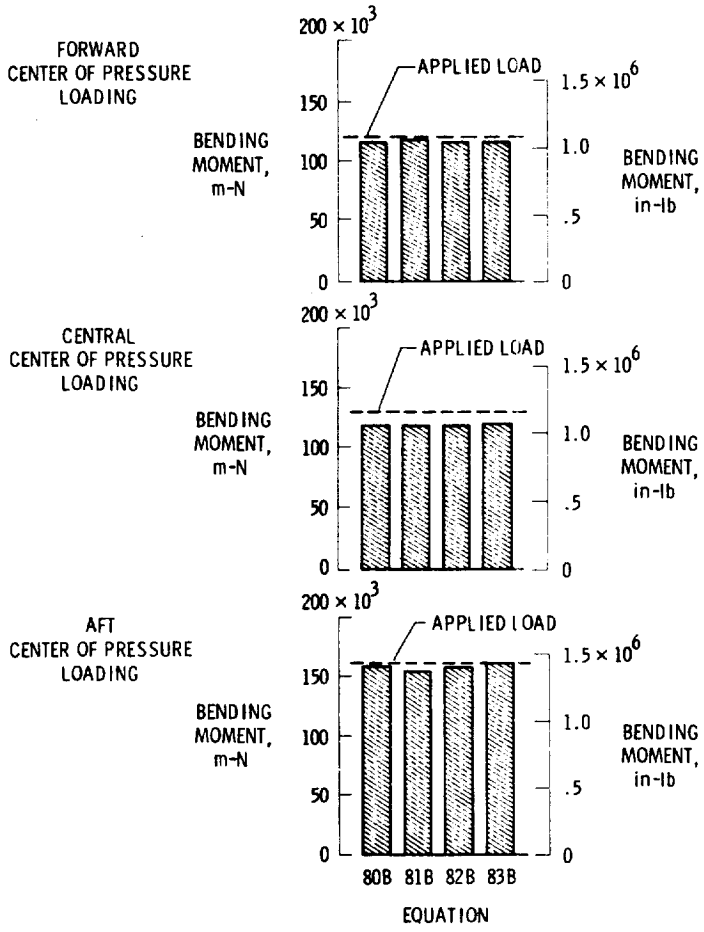

Figure 17

COMPARISON OF CALCULATED AND MATHEMATICALLY APPLIED TORSION LOADS

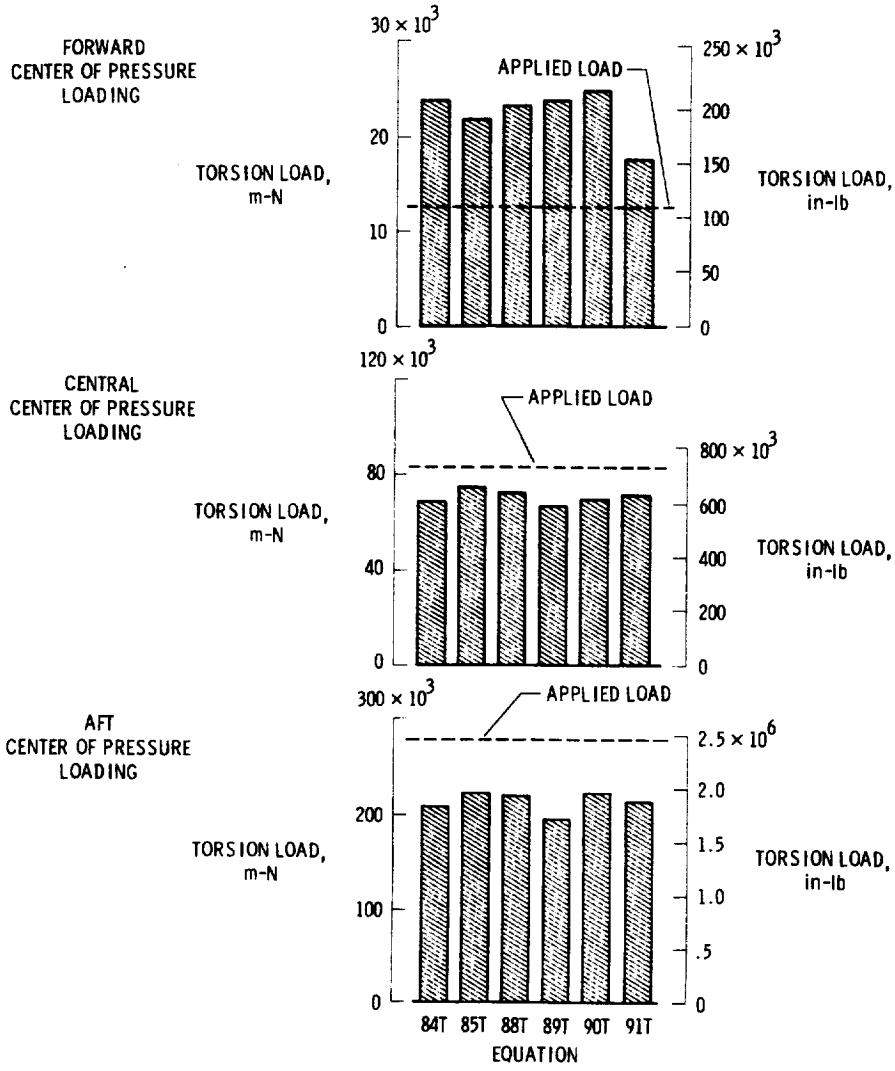

Figure 18

LOCATION AND RELATIVE MAGNITUDE OF LOADS APPLIED
DURING LOAD CALIBRATION

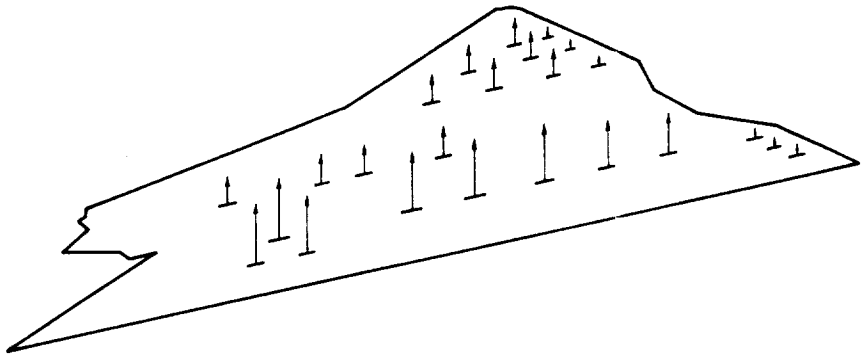

Figure 19

COMPARISON OF MEASURED AND CALCULATED SHEAR STRAINS
FOR SEVERAL DISCRETE LOADS

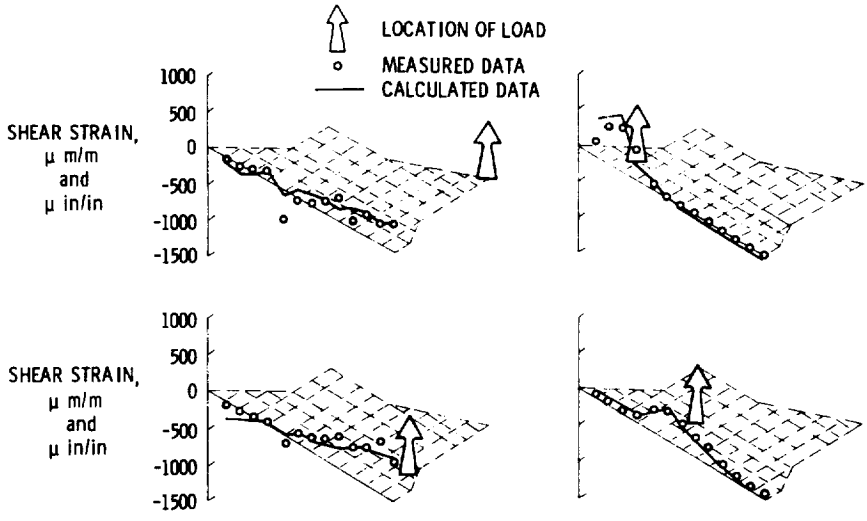

Figure 20

COMPARISON OF MEASURED AND CALCULATED BENDING STRAINS
FOR SEVERAL DISCRETE LOADS

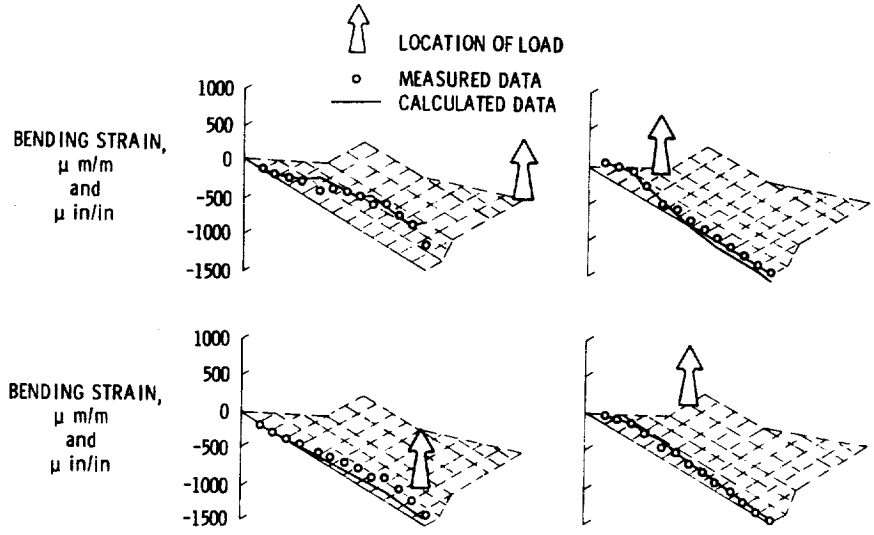

Figure 21

COMPARISON OF MEASURED AND CALCULATED INFLUENCE
COEFFICIENT PLOTS FOR SHEAR STRAIN

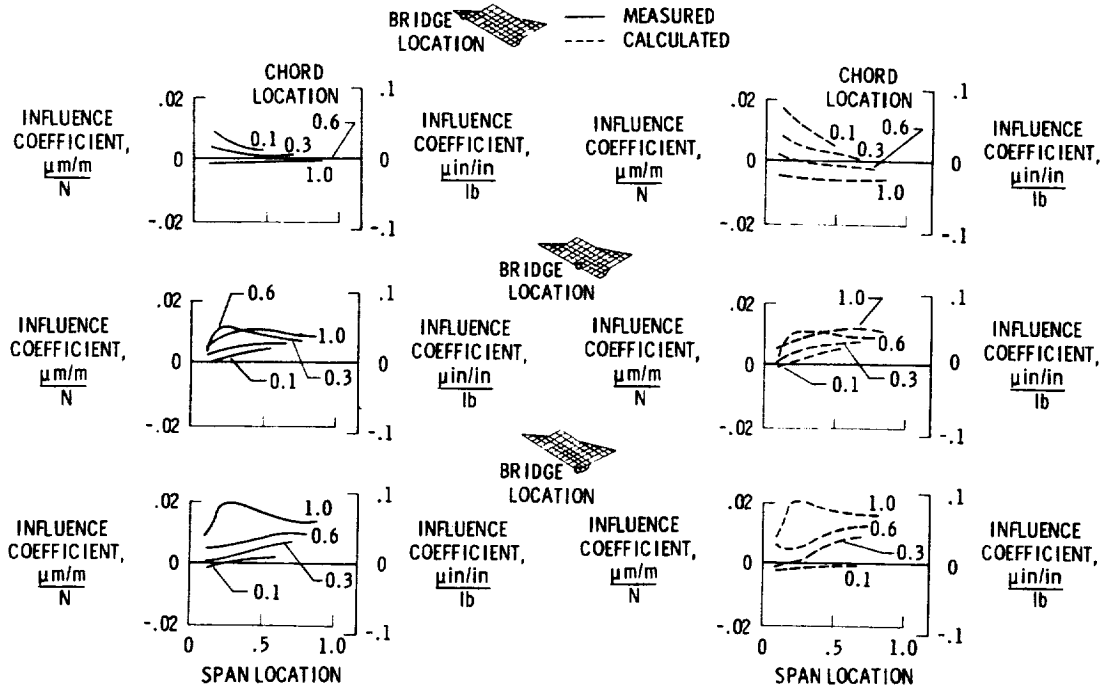

Figure 22

COMPARISON OF MEASURED AND CALCULATED INFLUENCE COEFFICIENT PLOTS FOR BENDING STRAIN

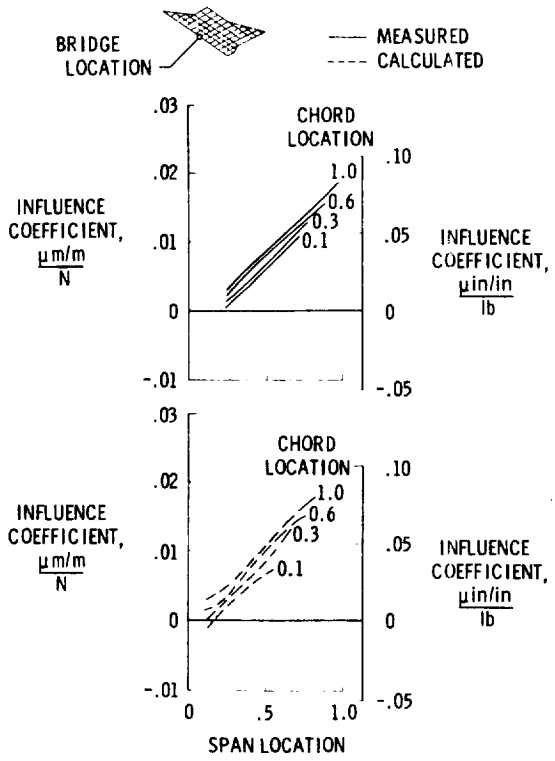

Figure 23